Nuclear quadrupole moment of ^{201}Hg

Jacek Bieroń,[1] Pekka Pyykkö,[2] and Per Jönsson[3]
[1]*Instytut Fizyki imienia Mariana Smoluchowskiego, Uniwersytet Jagielloński, Reymonta 4, PL-30-059 Kraków, Poland*
[2]*Department of Chemistry, University of Helsinki, P.O. Box 55 (A.I. Virtasen aukio 1), 00014 Helsinki, Finland*
[3]*Applied Mathematics Group, Malmö University, 205 06 Malmö, Sweden*
(Received 22 September 2004; published 6 January 2005)

The multiconfiguration Dirac-Hartree-Fock model has been employed to compute the magnetic dipole hyperfine structure constant and the electric field gradient in the $^3P_1$ state of neutral mercury. Combined with the experimental electric quadrupole hyperfine interaction constant, the computed electric field gradient yields the nuclear quadrupole moment $Q=387\pm6$ mb for ^{201}Hg. This value is in good agreement with older muonic, atomic, and solid-state values, but differs from the latest muonic result and from the recent γ spectroscopy determination.

DOI: 10.1103/PhysRevA.71.012502 PACS number(s): 31.30.Jv, 31.15.Ar, 31.30.Gs, 21.10.Ky

I. INTRODUCTION

Mercury has one stable quadrupolar isotope ^{201}Hg ($I=3/2$), with relative abundance 13.2%. The isotope ^{199}Hg, with relative abundance 16.9%, has two quadrupolar excited states at 158 and 208 keV. Values of the quadrupole moments for several radioactive isotopes with masses from 185 to 203 were reported by Ulm *et al.* [1]. A comprehensive compilation of the quadrupole moments for the isotopes in the mass range 185–206 was included in the tables of Raghavan [2]. Most of these data are based on the primary $Q(^{201}\mathrm{Hg})$ value, combined with measured isotopic ratios. A number of available experimental values [1,3–11] of the quadrupole moment Q of ^{201}Hg isotope are quoted in Table I of the present paper. The "muonic 3*d*" value of 386(49) mb was used in a recent "year-2001" summary [12] of nuclear quadrupole moments.

The electric quadrupole spectroscopic hyperfine constant B of an atomic state is related to the electric field gradient q and to the electric quadrupole moment eQ of the nucleus in the following way:

$$B = eqQ/h. \tag{1}$$

In the present paper we combine the available experimental hyperfine atomic data for ^{201}Hg [14] with the electric field gradient obtained from large-scale multiconfiguration Dirac-Hartree-Fock (MCDHF) calculations, to obtain a more accurate value of $Q(^{201}\mathrm{Hg})$. The same method has previously been applied to the nuclear electric quadrupole moments of other heavy elements, such as Br, I [15], and Bi [16].

II. THEORY

The multiconfiguration Dirac-Hartree-Fock method [17] was used in the present paper. Starting from the Dirac-Coulomb Hamiltonian

$$H_{DC} = \sum_i c\boldsymbol{\alpha}_i \cdot \boldsymbol{p}_i + (\beta_i - 1)c^2 + V_i^N + \sum_{i>j} 1/r_{ij}, \tag{2}$$

where V^N is the monopole part of the electron-nucleus Coulomb interaction, the wave function for an atomic state (ASF) was obtained as the self-consistent solution of the Dirac-Fock equation [18] in a basis of symmetry-adapted configuration-state functions (CSF's)

$$\Psi(\Gamma PJM) = \sum_j^{NCF} c_j \Phi(\gamma_j PJM). \tag{3}$$

The basis was systematically enlarged [16,19] to yield increasingly accurate approximations to the exact wave function. All calculations were done with the nucleus modeled as a variable-density sphere, where a two-parameter Fermi function [20] was employed to approximate the charge distribution. The magnetic dipole interaction constant A and the electric field gradient q were evaluated from the computed wave functions, using the HFS92 program [21]. The nuclear

TABLE I. Proposed values of nuclear electric quadrupole moment Q of ^{201}Hg in reverse chronological order.

Q (mb)	Method	Reference	Year
387 (6)	Atomic	This work	
347.0 (43.0)	Nuclear	Fornal *et al.* [3]	2001
385 (40)	Atomic[a]	Ulm *et al.* [1]	1988
485 (68)	Muonic[b]	Günther *et al.* [4]	1983
386 (49)	Muonic 3*d*[c]	Hahn *et al.* [5]	1979
267 (37)	Muonic 2*p*[c]	Hahn *et al.* [5]	1979
390 (20)	Solid[d]	Edelstein and Pound [6]	1975
455 (40)	Atomic $^3P_2$	McDermott and Lichten [7]	1960
420	Atomic	Murakawa [8]	1959
500 (50)	Atomic[e]	Blaise and Chantrel [9]	1957
600	Solid[e]	Dehmelt *et al.* [10]	1954
500	Atomic[e]	Schüler and Schmidt [11]	1935

[a]Standard value of Raghavan [2].
[b]Combines the $^{199}\mathrm{Hg}(I=5/2)$ value of [4] with the 201/199 ratio of [13].
[c]Direct muonic measurement on ^{201}Hg.
[d]Solid $HgCl_2$ plus ^{199}Hg nuclear primary value.
[e]Not Sternheimer corrected.

 ©2005 The American Physical Society

magnetic dipole moment for the $^{201}_{80}$Hg isotope was taken from the tables of Raghavan [2].

III. METHOD

The generation of the wave function was divided into four phases. In the first phase, the spectroscopic orbitals required to form a reference wave function were obtained with a minimal configuration expansion, with full relaxation.

In the second phase, the virtual orbitals were generated in four consecutive steps. At each step the virtual set was extended by one layer of virtual orbitals. A layer is defined as a set of virtual orbitals with different angular symmetries. In the present paper four layers of virtual orbitals of each of the s,p,d,f,g,h symmetries were generated. At each step the configuration expansions were limited to single and double substitutions from valence shells to all new orbitals and to all previously generated virtual layers (valence correlation approximation). These configuration expansions were augmented by small subset of dominant single and double substitutions from core ($5s5p5d$) and valence ($6s6p$) shells, with the further restriction that at most one electron may be promoted from core shells (which means that in the case of a double substitution the second electron must be promoted from a valence shell). All configurations from earlier steps were retained, with all previously generated orbitals fixed, and all new orbitals made orthogonal to others of the same symmetry. The initial shapes of radial orbitals were obtained in Thomas-Fermi potential and then driven to convergence with the self-consistency threshold set to 10^{-8}.

In the third phase, the configuration-interaction calculations (i.e., with no changes to the radial wave functions) were performed, with multiconfiguration expansions tailored in such a way as to capture the core polarization, which is the leading electron correlation contribution to the hyperfine expectation values [22–24]. All single and double substitutions were allowed from several core shells and all valence shells (i.e., $6s$, $6p-$, and $6p+$) to all virtual shells, with the same restriction as above—i.e., that at most one electron may be promoted from core shells (core-valence approximation). The virtual set was systematically increased from one to four layers. In a similar manner, several core shells were systematically opened for electron substitutions—from the outermost $5d$ to $3s3p3d$ shells. The substitutions from $3s$ shell changed the calculated value of magnetic dipole hyperfine constant A by less than 0.2%. The effect on electric field gradient was almost an order of magnitude smaller; therefore, no deeper core shells were opened. The contribution from the fourth layer of virtual orbitals to the calculated values of the magnetic dipole hyperfine constant A and the electric field gradient q turned out to be less than 1%. During generation of the fifth layer convergence problems were encountered with the s symmetry orbital. The contribution from the incomplete fifth layer of virtual orbitals to the calculated value of A was of the order of 0.1%, and 0.5% in the case of q. Based on our earlier hyperfine structure calculations [19,25], we estimate the core-valence contribution arising from all omitted shells to be of the order of a fraction of a percent.

In the fourth phase of the wave function generation the core-core correlation effects were estimated in a series of configuration-interaction calculations. First, the core $4s4p4d4f5s5p5d$ shells were systematically opened for double substitutions to one layer of virtual orbitals. At each step they were added to the final core-valence expansion. The double substitutions from the outermost core shells ($5s5p5d$) together brought about almost 10% change of the calculated value of A and 6% change of q. The effect of the deeper-lying core shells ($4s4p4d4f$) was almost an order of magnitude smaller. In the next step, the double substitutions from the core $5s5p5d$ shells were allowed to the full first layer of virtual orbitals and to the subset of the second layer (the subset comprised a virtual orbital of the symmetry s, p, or both), and again augmented by the final core-valence expansion. The effect of the substitutions to the (incomplete) second layer turned out to be a fraction of a percent for both A and q. At this point, the bulk structure of the core-core electron correlation had been revealed and all dominant effects were under control with 1% precision or better. The final, largest configuration-interaction calculation was composed of 158 534 configurations which were generated from (1) final core-valence expansion, (2) double substitutions from the core $4s4p4d4f5s5p5d$ shells to the full first layer of virtual orbitals, or (3) double substitutions from the core $5s5p5d$ shells to the first layer of virtual orbitals augmented by the subset (s and p symmetries) of the second layer. Each of the last few configuration-interaction calculations took between 1 and 2 weeks on an eight-node cluster of Linux machines of 13 GHz total peak power and required up to 100 GB temporary disk storage for the Hamiltonian matrix.

The Breit and QED corrections were estimated with the method described in [19], limited to a small-scale (3134 relativistic configurations) configuration-interaction calculation, where multiconfiguration expansions were limited to core-valence substitutions from the valence shells and the core $4f5s5p5d$ shells to one layer of virtual orbitals. The matrix elements of the Breit operator in the low-frequency limit

$$B_{ij} = -\frac{1}{2r_{ij}}\left[\boldsymbol{\alpha}_i \cdot \boldsymbol{\alpha}_j + \frac{(\boldsymbol{\alpha}_i \cdot \mathbf{r}_{ij})(\boldsymbol{\alpha}_j \cdot \mathbf{r}_{ij})}{r_{ij}^2}\right], \tag{4}$$

were evaluated perturbatively, as described in [26]. The QED effects included the anomalous magnetic moment of the electron, for which the factor $g_s/2 = 1.001\,159\,652\,19$ has been used [27], vacuum polarization, and self-energy [26].

The hyperfine structure Hamiltonian [21] assumes point-like nuclear dipole moments. The correction arising from spatial distribution of magnetic moment inside the nucleus (the Bohr-Weisskopf [28] effect) depends primarily on the radial shape of the magnetization distribution of ^{201}Hg, which is unknown. We employed the modified approach of Zemach [29], who evaluated the multiplicative correction factor arising from the magnetization distribution for states of s symmetry. In order to apply this correction, we separated the calculated value of the magnetic hyperfine constant A into *contact*, *spin-dipole*, and *orbital* terms, using the nonrelativistic MCHF formalism [30]. It turned out that the *contact* term yields approximately 80% of the total value of the cal-

TABLE II. Calculated values of the nuclear electric quadrupole moment Q (mb), the electric field gradient q (a.u.), and the magnetic dipole hyperfine structure constant A (MHz) of ^{201}Hg in various approximations, compared with experiment. DF: uncorrelated Dirac-Fock. vv (valence correlation): $6sp \rightarrow 4$ virtual layers. cv (core-valence): $3spd4spdf5spd6sp \rightarrow 4$ virtual layers. cc (core-core): $4spdf5spd6sp \rightarrow 1$ virtual layer$+5spd6sp \rightarrow 4/3$ virtual layers (see text for full descriptions).

Model	Q (mb)	q (a.u.)	A (MHz)
DF	478.713	2.49027	−4368.266
vv	380.549	−3.13264	−5846.665
vv+cv	359.056	−3.32016	−6216.632
vv+cv+cc	389.035	−3.06431	−5523.861
Breit & QED	−2.409	−0.01909	−20.739
Bohr-Weisskopf			+73.790
Total	386.626	−3.08340	−5470.810
Expt. [14]			−5454.569(0.003)

culated value of A. Therefore we applied the Zemach correction to the *contact* term alone and neglected contributions to Bohr-Weisskopf effect arising from other spherical symmetries [31]. This approximate procedure yields Zemach correction factor $1-\epsilon=0.987$, in qualitative agreement with $1-\epsilon=0.992$ reported by Kopfermann [32].

IV. RESULTS AND DISCUSSION

Table II shows the calculated values of the nuclear electric quadrupole moment Q of ^{201}Hg isotope, the electric field gradient q (a.u.), and the magnetic dipole hyperfine constant A of the $^3P_1$ state of neutral mercury. The left-hand side of Fig. 1 presents the dependence of the calculated value of the nuclear quadrupole moment Q on the size of the multiconfiguration expansion in the MCDHF model and shows the convergence towards the final value of Q. On the right-hand side of Fig. 1 our final value is compared with several recent results obtained with other methods (in reverse chronological order—the latest to the left). Only those experimental values are represented for which error limits had been published. Our calculated value of Q lies within the error bounds of the two latest experimental results and agrees quite well with one of them. As can be seen in Fig. 2, the experimental values themselves also exhibit a pattern of convergence, although relatively large error bars do not allow too far reaching conclusions, and tension still remains between the latest six results. The resolution of the differences was the prime objective of the present paper; therefore, in the last section we make an attempt to estimate the accuracy of the result of our calculations.

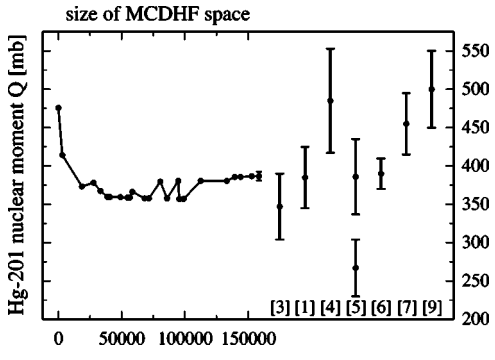

FIG. 1. The mercury-201 nuclear quadrupole moment Q as a function of the number of configuration functions in the multiconfiguration expansion, compared with experimental values (in reverse chronological order—the latest to the left). The numbers in square brackets indicate the literature references.

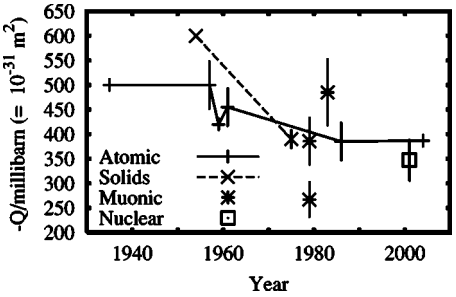

FIG. 2. The mercury-201 nuclear quadrupole moment Q as a function of time. Note the essential convergence of the 1975 solid-state, 1979 muonic, and present atomic values.

V. ERROR BUDGET

The error limit of the semiempirically determined value of the quadrupole moment Q arises from theoretical and experimental contributions. While the latter is directly scaled from the experimental error bar of the hyperfine constant B, establishing error bounds of *ab initio* computer simulations of many-body systems is a very difficult and risk-prone task. We envisaged three different methods, but no firm level of confidence can be established for any of them. They are discussed in the following subsections.

A. Extrapolation

The calculations presented in the present paper were based on the principle of the systematic expansions of the active set, as described in Sec. III. Systematic increase of the multiconfiguration expansion allows us to control the size of the active set and to monitor the convergence of the expectation value(s). In combination with the method of complete active set [33,34], this procedure permits also an extrapolation of the dependence of the calculated expectation values on the multiconfiguration expansion, at least for light atoms [35,36]. For a system as heavy as Hg, neither the complete active set nor fully systematic expansion is possible and one has to rely on stepwise procedures of the sort described in Sec. III. A rigorous extrapolation is not possible either. The only reasonable approach is a visual inspection of the graphs, in order to observe the convergence. To make an error estimate, one may identify the last "visible," non-negligible oscillation in Fig. 1 as a crude estimate of the error bar, pro-

vided that the oscillations are damped. This approach yields error limit $\Delta Q = 5.1$ mb.

B. Estimates of the error sources

The accuracy of the calculated value of the hyperfine magnetic dipole constant A and its dependence on the expansions employed in the core-valence model indicate that the core-polarization effects were fully accounted for. The same cannot be said about higher-order effects, though. The "core-valence + core-core" model certainly captured a large part of the core-core correlation, but the "core-core" configuration expansions rather do not guarantee saturation of the expectation values with respect to the core-core correlation. The computer limitations did not permit more extensive core-core configuration expansions and certain classes of substitutions were left out.

While it is difficult to precisely determine the magnitude of the uncaptured correlation effects, rough estimates of all possible sources of uncertainty were given in Sec. III, in percentage points. Translated into absolute values, they yield 2 mb from the incomplete fifth layer of virtual orbitals, 4 mb from the omitted core-valence substitutions, 8 mb from the omitted double substitutions, and 4 mb from the triple- and higher-order substitutions. The above estimates are rather conservative. The largest source of the uncertainty comes probably from the omitted double substitutions; our estimate was based on direct calculations for other, much lighter systems [15,19,25]. The relative contribution from (omitted in the present paper) triple- and higher-order substitutions has been taken from the (nonrelativistic) evaluations for bromine and iodine [15]. The root mean square of the above four estimates yields $\Delta Q = 5.8$ mb.

C. Relative accuracy of the hyperfine constant *A*

Both the experimental value of the magnetic dipole hyperfine constant A [14] and the nuclear magnetic dipole moment μ [2] had been measured at the ppm level, which allows making meaningful comparisons of the theoretically determined results. The accuracy of the calculated value of the electric field gradient q may be expected to be of the same order or better than the accuracy of the calculated value of magnetic dipole hyperfine constant A, for the following reasons: in the relativistic theory [37] the q operator depends on the $\langle r^{-3} \rangle$ expectation value, whereas the A operator depends on $\langle r^{-2} \rangle$; however, the latter mixes the great and small components of the radial wave function. Therefore, in the nonrelativistic approximation, both q and A depend on the $\langle r^{-3} \rangle$ expectation value, which makes them equally sensitive to the inner part of the radial wave function, where core-core correlation dominates the configuration-interaction effects. The A value depends on spin polarization effects, which makes it more sensitive than q to core-valence electron correlation effects. Neglecting for a while the experimental uncertainty (i.e., the contribution from the error bounds ΔB of the experimental value of the electric quadrupole hyperfine constant B), the following approximations may be inferred from the above considerations and Eq. (1):

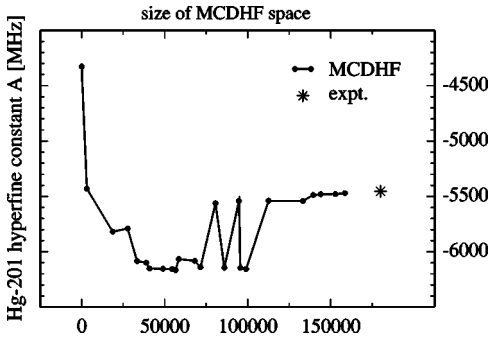

FIG. 3. The mercury-201 hyperfine magnetic dipole constant A as a function of the number of configuration functions in the multiconfiguration expansion, compared with experimental value [14].

$$\Delta Q/Q \approx \Delta q/q \approx \Delta A/A. \tag{5}$$

The calculated value of A in several different approximations is presented in the last column of the Table II and compared with the experimentally determined value [14]. Figure 3 shows the dependence of the calculated value of A on the size of the multiconfiguration expansion in the MCDHF model. The points in Fig. 3 are corrected for Breit, QED, and Bohr-Weisskopf effects. The relative accuracy $\Delta A/A = 0.003$ is very impressive and yields, via Eq. (5), the error limit $\Delta Q = 1.2$ mb. It can be taken as a confirmation that the theoretical model adopted in the present paper correctly describes the dominant correlation effects. However, experience from previous calculations of hyperfine structures and electromagnetic moments of heavy elements [15,16,19,25] indicates that agreement this close is very likely accidental; therefore, the estimate based on Eq. (5) should not be considered as a reliable determination of the accuracy of the calculated value of Q.

D. Accuracy of the hyperfine constant *B*

The hyperfine structure constants A and B were determined by Kohler [14]. The stated error limit of the experimental value $B = -280.107 \pm 0.005$ MHz translates into the experimental contribution $\Delta Q = 0.007$ mb, which is negligible in comparison with the theoretical uncertainty.

E. Total error estimate

The largest of the above estimates of the theoretical uncertainty (Sec. V B) yields the following electric quadrupole moment for the ^{201}Hg nucleus:

$$Q = 387 \pm 6 \text{ mb}.$$

VI. CONCLUSIONS

Neglecting small-scale differences, a striking resemblance of the overall shapes of the curves presented in Figs. 1 and 3 is worth noting. It supports the conclusion drawn above that both q and A are equally sensitive to electron correlation effects. Should this trend continue, it would be tempting to assume that the quadrupole moment should asymptotically

arrive at the value $Q=387.78$ mb (with error limit set by the numerical accuracy), but the assumption is not true in general.

As seen from Table I and Figs. 1 and 2, the 1979 "muonic $3d$" value by Hahn *et al.* [5], the latest solid-state, and the atomic values of the $Q(^{201}\mathrm{Hg})$ agree rather well with each other and with the present MCDHF value. Among the latest results the 1983 "muonic" value [4], the 1979 "muonic $2p$" value [5], and the 2001 "nuclear" (γ-ray) determination [3] deviate most from our value. The present MCDHF value of $Q(^{201}\mathrm{Hg})$ is in very good agreement with the standard value of Raghavan [2], as well as with the value quoted in the "year-2001" summary [12]. Therefore our calculations confirm the previously adopted standards but reduce the error limits from the 10% range to the 2% range, a fivefold improvement.

ACKNOWLEDGMENTS

This research has been supported by KBN Grant No. 2 P03B 051 22 and Academy of Finland Grant Nos. 200903 and 206102.

[1] G. Ulm *et al.*, Z. Phys. A **325**, 247 (1986).
[2] P. Raghavan, At. Data Nucl. Data Tables **42**, 189 (1989).
[3] B. Fornal *et al.*, Phys. Rev. Lett. **87**, 212501 (2001).
[4] C. Günther, E. B. Shera, M. V. Hoehn, H. D. Wohlfart, R. J. Powers, Y. Tanaka, and A. R. Kunselman, Phys. Rev. C **27**, 816 (1983).
[5] A. A. Hahn, J. P. Miller, R. J. Powers, A. Zehnder, A. M. Rushton, R. E. Welsh, A. R. Kunselman, P. Roberson, and H. K. Walther, Nucl. Phys. A **314**, 361 (1979).
[6] W. A. Edelstein and R. V. Pound, Phys. Rev. B **11**, 985 (1975).
[7] M. N. McDermott and W. L. Lichten, Phys. Rev. **119**, 134 (1960).
[8] K. Murakawa, J. Phys. Soc. Jpn. **14**, 1624 (1959).
[9] J. Blaise and H. Chantrel, J. Phys. Radium **18**, 193 (1957).
[10] H. G. Dehmelt, H. G. Robinson, and W. Gordy, Phys. Rev. **93**, 480 (1954).
[11] H. Schüler and T. Schmidt, Z. Phys. **98**, 239 (1935).
[12] P. Pyykkö, Mol. Phys. **99**, 1617 (2001).
[13] W. Tröger, T. Butz, P. Blaha, and K. Schwarz, Hyperfine Interact. **80**, 1109 (1993).
[14] R. H. Kohler, Phys. Rev. **121**, 1104 (1961).
[15] J. Bieroń, P. Pyykkö, D. Sundholm, V. Kellö, and A. J. Sadlej, Phys. Rev. A **64**, 052507 (2001).
[16] J. Bieroń and P. Pyykkö, Phys. Rev. Lett. **87**, 133003 (2001).
[17] I. P. Grant, Comput. Phys. Commun. **84**, 59 (1994).
[18] F. A. Parpia, C. Froese Fischer, and I. P. Grant, Comput. Phys. Commun. **94**, 249 (1996).
[19] J. Bieroń, P. Jönsson, and C. Froese Fischer, Phys. Rev. A **60**, 3547 (1999).
[20] K. G. Dyall, I. P. Grant, C. T. Johnson, F. A. Parpia, and E. P. Plummer, Comput. Phys. Commun. **55**, 425 (1989).
[21] P. Jönsson, F. A. Parpia, and C. Froese Fischer, Comput. Phys. Commun. **96**, 301 (1996).
[22] C. Froese Fischer, T. Brage, and P. Jönsson, *Computational Atomic Structure: An MCHF Approach* (Institute of Physics, London, 1997), pp. 171–173.
[23] B. Engels, Theor. Chim. Acta **86**, 429 (1993).
[24] J.-L. Heully and A.-M. Mårtensson-Pendrill, Phys. Scr. **31**, 169 (1985).
[25] J. Bieroń, P. Jönsson, and C. Froese Fischer, Phys. Rev. A **53**, 2181 (1996).
[26] B. J. McKenzie, I. P. Grant, and P. H. Norrington, Comput. Phys. Commun. **21**, 233 (1980).
[27] URL physics.nist.gov/cuu/Constants/index.html
[28] A. Bohr and F. Weisskopf, Phys. Rev. **77**, 94 (1950).
[29] A. C. Zemach, Phys. Rev. **104**, 1771 (1956).
[30] C. Froese Fischer, T. Brage, and P. Jönsson, *Computational Atomic Structure: An MCHF Approach* (Institute of Physics, London, 1997), pp. 165–166.
[31] A.-M. Mårtensson-Pendrill, Phys. Rev. Lett. **74**, 2184 (1995).
[32] H. Kopfermann, *Nuclear Moments* (Academic, New York, 1958).
[33] B. O. Roos, R. P. Taylor, and P. E. M. Siegbahn, Chem. Phys. **48**, 157 (1983).
[34] J. Olsen, P. Jørgensen, H. J. A. Jensen, and B. O. Roos, J. Chem. Phys. **89**, 2185 (1988).
[35] M. Tong, P. Jönsson, and C. Froese Fischer, Phys. Scr. **48**, 446 (1993).
[36] D. Sundholm and J. Olsen, Phys. Rev. A **42**, 2614 (1990).
[37] I. Lindgren and A. Rosén, Case Stud. At. Phys. **4**, 93 (1974).